The OpenQuake Book

Version 1.0

"OpenQuake: Shaken not stirred"

The OpenQuake Book

Authors:
Helen Crowley[1], Leonardo Garrido[1], Damiano Monelli[3], Marco Pagani[1], Vitor Silva[2], Graeme Weatherill[2]

[1] GEM Foundation
via Ferrata, 1
20133 Pavia
Italy

[2] GEM Model Facility
via Ferrata, 1
20133 Pavia
Italy

[3] GEM Model Facility
SED - ETHZ
Sonneggstrasse, 5
CH-8092 Zurich
Switzerland

Email address (for all the authors):
<name.surname>@globalquakemodel.org

Contents

Symbols and acronyms

Quantity or Description	Symbol or acronym	Unit of measure
Distance	D or d	km
Frequency-Magnitude Distribution	FMD	
Gutenberg-Richter (frequency-magnitude distribution)	G-R	
Ground motion (GM) or intensity measure type (IMT)	U or u	g
Ground Motion Field	GMF	
Ground Motion Prediction Equation	GMPE	
Ground Motion Prediction Equation System	GMPES	
Magnitude	M or m	
Natural hazards' Risk Markup Language	nrML	
Occurrence Rate	λ	events/yr
OpenQuake	OQ	
Rupture	rup	
Seismic Source System	SSS	
Stochastic Event Set	SES	

PART I

Introduction

CHAPTER 1

OpenQuake background

An OpenQuake schema evidencing main inputs and calculators is represented in Figure 1.1.

Figure 1.1.: OpenQuake schema. Purple boxes are the calculators included in the the hazard part of OQ; green boxes are the risk calculators. The method of Wesson et al. [2009] is represented in a separate box since it incorporates hazard and risk calculations.

CHAPTER 2

Brief desciption of OpenQuake IT aspects

2.1. Risk-lib

PART II
Hazard

CHAPTER 3

Introduction

Probabilistic Seismic Hazard is nowadays a well established methodology, largely founded on the works of Cornell and Esteva, both published at the end of the 1960's. The development of PSHA within the latest four decades did not change much the original concept but made calculations more rigorous and accurate, especially with respect to the treatment of uncertainties.

The evolution of PSHA methodologies proceeded in parallel with the development of instrumental seismology and hardware computing power. Computer codes such as EQRISK [McGuire, 1976] and different SEISRISK versions [Bender and Perkins, 1982, 1987] traced the advancement of PSHA calculation within the last part of the 20th century.

At the present time, the most computationally intensive PSHA models available are the ones developed for site-specific PSHA analyses, such as the ones performed for special installations, and the regional PSHA input models. In the first case most of the computetion demand comes from the complexity of the input whilst in the second case is the number of sites considered that makes calculations particularly heavy.

3.1. OpenQuake-hazard: main concepts

OpenQuake-hazard leverages from OpenSHA (http://www.opensha.org) - an open-source, Java-based platform for conducting Seismic Hazard Analysis - and it is developed in collaboration with the OpenSHA team.

Schematically, the procedure OpenQuake follows to compute the hazard is the following:

1. *Read the PSHA input model - i.e. the union of the Seismic Sources System and the GMPE system - and calculation settings.*

   The Seismic Source System is an object that contains the information necessary to create one or several Source Model, eventually by taking into account the epistemic uncertainties. In particular, the Seismic Sources System contains:

- One or several Initial Source Models (ISMs);
- One logic tree - the Seismic Source logic tree - describing epistemic uncertainties connected with the objects and parameters characterizing the initial source models.

The GMPEs System is an object that contains the information necessary to create one or several GMPE model, eventually by taking into account the epistemic uncertainties.

- One or several GMPES (ISMs);
- One logic tree - the Ground Motion Prediction Equations logic tree - describing epistemic uncertainties connected with the objects and parameters characterizing the selected GMPEs.

2. *Process the logic tree structures to account for epistemic uncertainties connected with the seismic sources and the ground motion prediction equations and create Source Models (SMs) and Ground Motion Prediction Equations Models (GMPEM).*

   A Source Model contains the information necessary to create an Earthquake Rupture Forecast (i.e. probabilistic seismicity occurrence model) without considering epistemic uncertainties.

   A Ground Motion Prediction Equation Model includes the information necessary to compute hazard using a source model.

3. Compute the hazard considering as many Source Models and Ground Motion Models as need to adequately characterise uncertainties.

4. Post-process the results obtained for distinct calculations.

CHAPTER 4

OpenQuake input description

An OpenQuake PSHA input model contains three distinct information blocks organised in two main objects: the Source System and the GMPEs System.

These information blocks include: (1) data regarding location, geometry, and seismicity properties of seismic sources, (2) details about ground motion prediction equations to be adopted in the calculation, (3) information about the epistemic uncertainties related to the two aforementioned points. A fourth separate, but important, chunk of information being part of the input are calculation settings.

OpenQuake PSHA input models are always defined using two logic tree structures where properties are specified branching level by branching level. In particular, OpenQuake requires two logic-tree structures, one describing epistemic uncertainties associated with the creation of the ERF - called Seismic Source logic tree - and one considering the uncertainties connected with the use of GMPEs - called GMPE logic tree. In cases when epistemic uncertainties are non accounted for, the logic tree structure simply consists of one branching level with just one branch (with weight equal to 1). Further explanations about the way we describe and model logic-trees are provided in section 4.1 at page 20.

OpenQuake currently support four types of seismic sources. The description of their main properties - subdivided into source location and geometry and source frequency-magnitude distribution - is provided in Section 4.2.1.

The selection of ground motion prediction equations (GMPE) in OpenQuake is basically accomplished by specifying a label in a particular file. The user can associate a GMPE to each tectonic region considered in the analysis (Active Shallow tectonic, Stable Continental etc.). Examples of GMPEs selection are provided in section 4.3 at page 26.

The last, but not less important, block of information characterizing a PSHA input model contains calculations settings i.e. parameters specifying the way calculations must be carried out. The information to be included in this part of the input is strictly related to the properties of the engine. Section 4.4 provides an outlook of the hazard specific calculation setting supported by OpenQuake.

4.1. Logic-tree description

Logic-trees are a tool designed to consider in a systematic manner the epistemic uncertainties of models and parameters included in a hazard analysis. In OpenQuake, the

Branching level definition: .... Simple Fault Dip Angle
Branching level uncertainty type: .... Absolute values
Applies to: .... Simple faults
Correlated branches: .... Yes

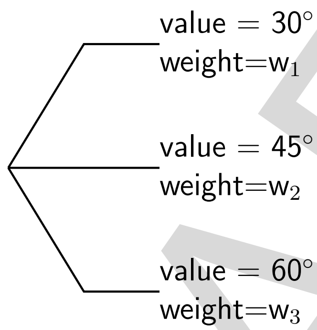

Figure 4.1.: Branching level description example. The upper example shows a branching level describing epistemic uncertainties on faults dip angle

description of a logic-tree structure uses as its principal component a branching level where a branching level consists on (1) the definition of the parameter - or elements - affected by uncertainty, (2) the specification of the type of uncertainty (3) the listing of the - mutually exclusive and collectively exhaustive [Bommer and Scherbaum, 2008] - alternative hypotheses and, (4) the index of the branches of the previous level - or the subset of seismic sources- to which this branching level applies. Each hypothesis (i.e. branch) included in a branching level has an associated value and a corresponding weight expressing - according to different interpretations available in the literature - "probabilities or simply subjective indications of relative merit" [Bommer and Scherbaum, 2008, page 999].

Figure 4.1 depicts an example of a branching level defining epistemic uncertainties on the dip angle of simple fault sources. In this case the possible values of the dip are specified on each branch composing the branching level (i.e. 30, 45 and 60 degrees). This means that these three values are the only ones admitted for all the sources included in the Source Model considered in this example.

Branching level definition: ....Simple Fault Dip Angle
Branching level uncertainty type: .... Relative values
Applies to: .... All previous branches
Correlated branches: .... Yes

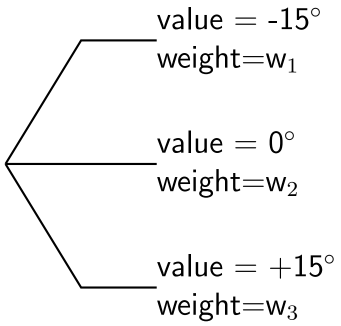

Figure 4.2.: Branching level description example. The upper example shows a branching level describing epistemic uncertainties on faults dip angle

Figure 4.2 shows a second example of a branching level defining epistemic uncertainties on the dip angle of simple fault sources. In this case the values specified for each branch aren't absolute dip angles but instead delta values to be added - or subtracted - to the initial dip value specified for each simple fault source contained in the initial source model. Once two or more branching levels are defined, in flexible fashion they can be combined (i.e. concatenated) to create an entire logic-tree structure. Figure 4.3 shows an example of a logic tree structure obtained by combining two branching levels described in the upper part of the figure. The first branching level accounts for epistemic uncertainties connected with the dip of simple fault sources whilst the second branching level specifies the epistemic uncertainties relative to the depth to the top of rupture for (this branching level also applies to simple faults included in the model). We use this logic tree description to specify the structure of the Seismic Source Logic Tree as well as for the Ground Motion Prediction Equation Logic Tree.

marco: we probably need abstract classes for all these components of the LT structure

4.2. OpenQuake seismic source typologies

A PSHA input model - excluding memory resources constraints - contains an unlimited number of sources specified in agreement with the typologies supported by OpenQuake. Each source type supported by OpenQuake is described by a limited numeber of parameters; in the following sections we provide a detailed description of the source typologies currently supported.

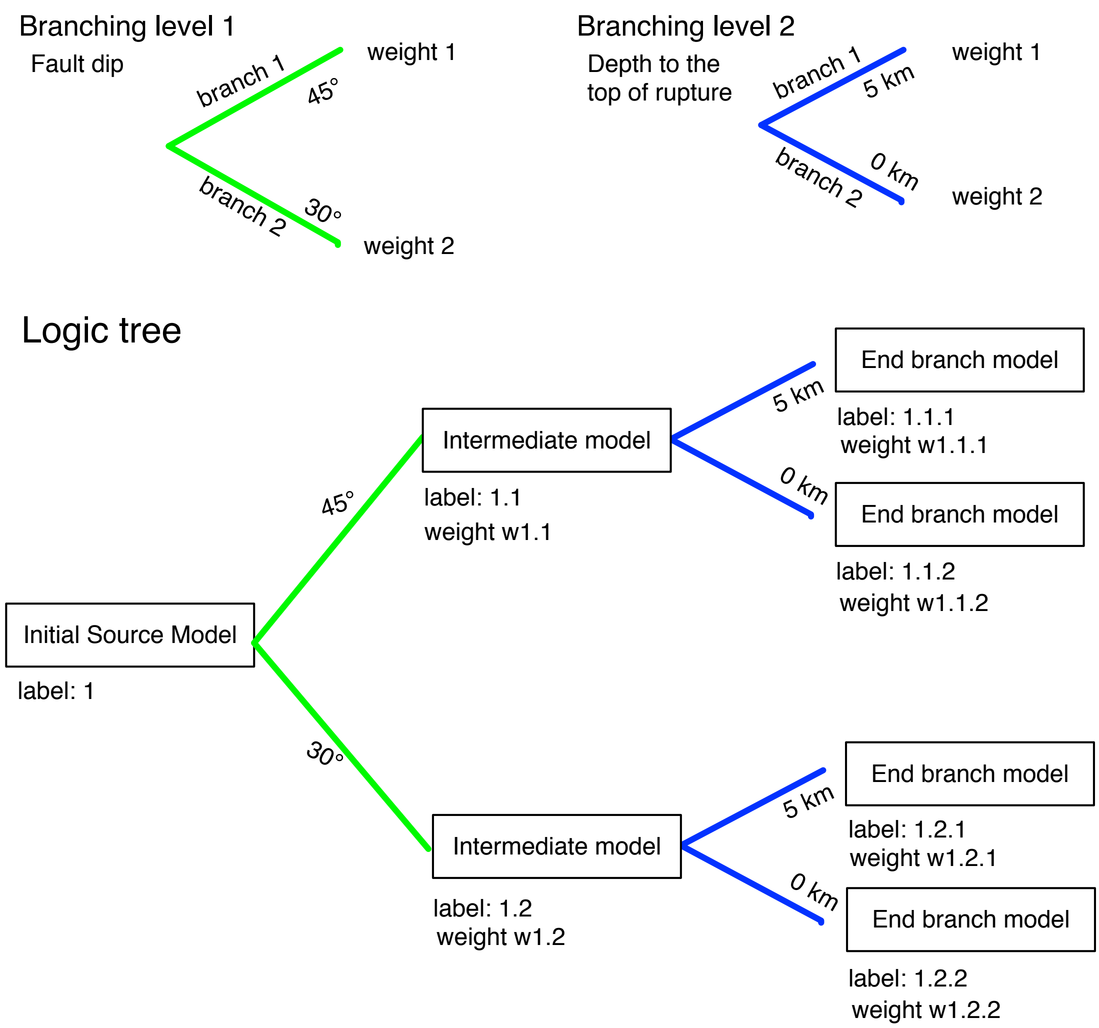

Figure 4.3.: Example of a logic tree structure as defined in OpenQuake. The upper part of the Figure depicts two branching levels.

4.2.1. Seismic source typologies description

OpenQuake, at present time, provides four seismic source typologies, for the most part defined in the course of the GEM1 project [Pagani et al., 2010]. These are:

- Area source - So far, the most frequently adopted source type in national and regional PSHA models.
- Grid source - Grid sources can be considered a replacement for area sources since they both model distributed seismicity;
- Simple fault sources - Simple faults are the easiest way to to specify a fault source in OpenQuake. This typology is usually adopted to describe shallow seismogenic fault sources.
- Complex fault sources - Complex faults are habitually adopted to model subduction interface sources with a complex geometry.

These are the basic assumptions accepted in the definition of these source typologies:

- In the case of area and fault sources, the seismicity is homogeneously distributed over the source;
- Seismicity temporal occurrence follows a Poissonian model;
- The frequency-magnitude distribution can be approximated to an evenly discretized distribution.

4.2.1.1. Area sources

Area sources model the seismicity occurring over wide areas where fault sources identification or characterization - i.e. unambiguous definition of seismicity occurrence parameters - is difficult.

The Senior Seismic Hazard Analysis Committee [1997] defined three main types of area seismic sources using as a discriminant their extension:

1. Area sources enclosing concentrated zones of seismicity;
2. Regional area sources;
3. Background area sources.

The criteria adopted for their definition - and the related uncertainties - vary according to each area source type. From a hazard computation standpoint we do not introduce any difference between these three area types.

marco: In the future we may support a specialized background area source type

Parameters

- A polygon that identifies the external border of the area. Eventually, internal borders can be specified so as to create holes inside an area [The current version of OQ doesn't support the definition of internal borders]
- One (or many) combinations of the following objects:
  - A discrete Frequency-Magnitude Distribution (FMD)
  - (optional) Strike, dip, and rake angles characterizing the seismicity in the corresponding FMD. For example, Coppersmith et al. [2009] defines a discrete distribution of strike values (dip is not considered because the source-site metrics they use is the Joyner-Boore distance).

  This description permits the accurate characterization of seismicity occurrence within an area by explicitly distributing the seismicity on the existing faulting trends.
- An array specifying the depth to the top of rupture dependency on magnitude. The array contains two columns and one or many <depth, magnitude> tuples. Each tuple specifies the depth to the top of rupture for magnitudes equal or greater than the corresponding value.
- A value to indicate the hypocentral depth in case of punctual sources. By convention all the events with magnitude lower than the lowest value of magnitude contained in the depth to the top of rupture array are modelled as punctual source. On the opposite, ruptures with magnitude equal or greater than the lowest value of magnitude contained in the depth to the top of rupture array are modelled considering their finite dimensions. The finite dimension of the rupture is computed using a magnitude-area or magnitude-length relationship specifies in the calculation settings file (in future versions of OQ we will allow the user to specify for each tectonic region the corresponding magnitude-scaling relationship).

4.2.1.2. Grid sources

A grid source is a typology used to model distributed seismicity - usually of low and intermediate magnitude. Grid sources can be considered a PSHA source model alternative to area sources, since they both try to represent distributed seismicity. Grid sources usually derive from the application of seismicity smoothing algorithms [Frankel, 1995; Woo, 1996]. The use of these algorithms carries some advantages compared to area sources, indeed, (1) they remove most of the unavoidable degree of subjectivity due to the definition of the geometries and (2) they define a seismicity spatial pattern that is, usually, more similar to reality. Nevertheless, some smoothing algorithms require the a-priori definition of some setup parameters that expose the calculation to a certain partiality level.

Grid sources are modelled in OpenQuake simply as a set of point sources. The next section describes the parameters required to characterize a point source.

Parameters

For each grid node:

- A location specified in terms of the <latitude,longitude> tuple;
- Similarly to area sources, one (or many) combinations of the following objects:
  - A discrete Frequency-Magnitude Distribution (FMD)
  - Strike, dip, and rake angles characterizing the seismicity specified in the associated FMD.
- An array to specify the dependency on magnitude of the depth to the top of rupture. This array contains two columns and one or many <depth, magnitude> tuples where each tuple specifies the depth to the top of rupture for magnitudes equal or greater than a specific value.
- A value to indicate the hypocentral depth in case of punctual sources. The same convention specified for area sources applies here.

4.2.1.3. Simple faults

Simple Faults are the most common source type used to model faults; the "simple" adjective relates to the geometry description of the source which is basically obtained by projecting a trace (i.e. a polyline) along a representative dip direction.

Parameters

- A fault trace (usually a polyline);
- A FMD;
- A representative value of the dip angle (specified according to the Aki-Richards convention; see Aki and Richards [2002]);
- Rake angle (specified following the Aki-Richards convention; see Aki and Richards [2002])

- Upper and lower values of depth limiting the seismogenic interval
- A boolean flag that specifies if the size of ruptures should follow a magnitude scaling relationship (currently specified in the calculation settings file) and be distributed homogeneously over the fault surface or it is accepted that ruptures within a given range of magnitudes (specified by the FMD) will always rupture the entire fault surface.

4.2.1.4. Complex faults

Complex faults differ from simple fault just by the way geometry is described and, consequently in the way the fault surface is created. The input parameters used to describe complex faults are, for the most part, the same used to describe the simple fault typology. In particular, in the case of complex faults the dip angle is not requested while the fault trace is substituted by two fault traces used to limit at top and bottom the fault surface.

Representation of complex faults

Usually, we use complex faults to model intraplate megathrust faults such as the big subduction structures active in the Pacific (Sumatra, South America, Japan).

4.3. GMPEs description

OpenQuake provides only hardcoded Ground Motion Prediction Equations and misses of a mechanisms allowing the user to specify new GMPEs. This is something the OpenQuake team may think to introduce in the future.

For the time being the user in need of a specific Intensity Measure Relationship, can:

- Fork the OpenQuake project from the OQ repository[1], code the new GMPE following the examples available in the OpenQuake and OpenSHA repository and, - if he's willing to share his contribution with the other OQ users - ask to push his modified version of OpenQuake.
- Post a ticket on the OpenQuake website

this is something I need to check with Ben

Table 4.1 provides a list of the Ground Motion Prediction Equations supported. The vast majority are GMPEs implemented in OpenSHA with just a couple of developed

Ground Motion Prediction Equation	IMTs	Component type	ID
Atkinson and Boore [2006]	PGA		AtkBoo06
Abrahamson and SIlva [2008]	PGA		AS2008
Boore and Atkinson [2008]	PGA,PGV,S$_a$	Avg Hor	BA2008
Chiou and Youngs [2008]	PGA,S$_a$		CY2008
Zhao et al. [2006]	PGA,S$_a$		ZhaoEtAl2006

Table 4.1.: Some of the Ground Motion Prediction Equations (in the OpenSHA terminology Intensity Measure Relationship) currently included in OpenSHA and OpenQuake.

in the course of the GEM1 project. New GMPEs are expected to be added soon with the contribution of some GEM's Regional Programmes.

4.4. Calculation settings description

[1] The OpenQuake software repository can be reached here: https://github.com/gem/openquake/

CHAPTER 5

Processing the Source Model Logic Tree and the calculation of the Earthquake Rupture Forecast

The calculation of the Seismicity Occurrence Model (i.e. ERF) starts from a Source model. The creation of a Source Model in OpenQuake is done by a calculator, named Logic Tree Processor (LTP). The LTP uses one of the ISMs and the logic tree structure included in the Source System to create Source Model. A Source Model is a complete description of the type, geometry and seismicity occurrence properties of the seismic sources necessary to calculate comprehensively the hazard over the investigated area. In a Source Model is not possible to inc epistemic uncertainties.

Once a Source Model is created, using the Earthquake Rupture Forecast calculator we create a list of the ruptures that can be generated by all the sources included in the Source Model. Each rupture is associated with a probability of occurrence in the time span specified in the calculation settings.

The Earthquake Rupture Forecast calculator creates computes for each rupture the probability of occurence in a time span specified in the configuration file. The list of ruptures correponds to all the possible ruptures that can be generated by the all the seismic sources included in Source Model can generate. Each rupture has

5.1. The Logic Tree processor

Logic Tree processor

5.2. ERF calculator

5.2.1. ERF creation in case of Grid sources

Area sources (see also Section 4.2.1.1 at page 23)

5.2.2. ERF creation in case of Grid sources

5.2.3. ERF creation in case of Fault sources

5.2.3.1. Fault sources with simple geometry

5.2.3.2. Fault sources with complex geometry

CHAPTER 6

Classical PSHA calculator

OpenQuake computes classical PSHA [Cornell, 1968; McGuire, 2004] following the methodology presented by Field et al. [2003]. This methodology has the distinctive property of performing the entire calculation using probabilities, as originally proposed by Chiang et al. [1984], instead of working with occurrence rates like in most of the commonest PSHA codes [see for instance Bender and Perkins, 1987]. The OpenSHA methodology has also the clear advantage of decoupling the creation of the probabilistic seismicity occurrence model (in the OpenSHA terminology this is defined as the Earthquake Rupture Forecast) from the assumption of a Poissonian temporal occurrence model.

As demonstrated by Field et al. [2003] - under the the assumption that the contribution to hazard coming from multiple occurrences occurring on a given seismic source is negligible i.e. the probability that a source will generate two or more occurrences within the time span fixed for the analysis is equal to zero - the calculation of hazard following this methodology is completely consistent with the most classical procedure. Pagani and Marcellini [2007] proved that this assumption holds at least for some prototypal situations.

Two are the main steps composing the OpenSHA seismic hazard calculation procedure:

- Creation of the probabilistic seismicity occurrence model, i.e. a discrete distribution giving the probability of occurrence - in a given time span - of each possible rupture occurring on one of the seismic sources defined in the PSHA input model. This step of the procedure was already discussed in Chapter 5 at page 29.

- Calculation of hazard at the site by combining the probabilistic seismicity occurrence model with a ground motion prediction equation (also Intensity Measure Relationship in the OpenSHA jargon). This second step will be the topic of the current chapter.

6.1. Hazard calculation: traditional formulation in terms of probabilities

In the simplest case, the classical PSHA calculation kernel takes as an input:

- An Earthquake Rupture Forecast (ERF - also called Probabilistic Seismicity Occurrence Model). An ERF is a list of all the possible ruptures occurring on all the seismic sources included in a Source Model. Each rupture Rup is associated with a probability of occurrence $P(Rup|t)$ referred to the time span t fixed for the analysis.
- A Ground Motion Prediction Equation (GMPE). A GMPE is an equation that - given some fundamental parameters characterizing the source, the propagation path and the site (in the simplest case magnitude, distance and $\mathrm{V}_{\mathrm{S},30}$) - computes the value GM of a (scalar) parameter describing ground motion intensity. gm is always accompanied by a standard deviation value $\sigma_{gm,T}$ specifying the aleatoric variability associated to gm.

Following Field et al. [2003], the exceedance of a value probabilities :

$$P(U \geq u) = 1 - \prod_{i=1}^{l} \left[\sum_{s=0}^{+\infty} \left(P(S=s) \left(1 - \sum_{j=0}^{j(i)} \sum_{s=0}^{K(i,j)} P(m_{i,j}) P(R_{i,j,k}|m_{i,j}) P(U \geq u | m_{i,j}, R_{i,j,k}) \right) \right) \tag{6.1}$$

where l i the number of sources

If the probability of multiple occurrences is assumed to be negligible the probability to get an exceedance of x in a given time span corresponds to:

$$P(X \geq x) = 1 - \prod_{i=1}^{l} \left(1 - \sum_{n=1}^{N(i)} P(Rup_{i,n}) P(X \geq x | Rup_{i,n}) \right) \tag{6.2}$$

6.1.1. Example

In case of two punctual sources each one generating a single rupture, the probability of exceedance of ground motion u in a given site corresponds to:

$$\begin{aligned} P(U \geq u) = 1 - \Big(& \left[1 - P(Rup_{i,1}) P(U \geq u | Rup_{i,1}) \right] \\ & \left[1 - P(Rup_{i,2}) P(U \geq u | Rup_{i,2}) \right] \Big) \end{aligned} \tag{6.3}$$

CHAPTER 7

Stochastic event set and ground motion field calculators

The calculation of stochastic event sets and the corresponding ground motion fields is a methodology tightly connected with a specific seismic risk analysis of common use within the insurance and re-insurance industry (CITATION).

OpenQuake - given a Source System - can generate a number of seismicity histories, each one representing a possible realisation of the seismicity that the sources included in a Source Model can generate within a given time span (fixed by the user). The

Each rupture in a seismicity history is successively associated with a ground motion field, an object describing the spatial distribution of a scalar parameter representative of the intensity of shaking (e.g. PGA or Spectral Acceleration). OpenQuake has the capability to generate

7.1. Stochastic Event Set Calculator

OpenQuake generates Stochastic Event Sets using the Inverse Trasform Sampling technique, probably the simplest and commonest methodology used to randomly sample probabily distribution starting from its cumulative form.

7.2. Ground Motion Fields calculator

We generate ground motion fields using the

7.2.1. Spatially correlated ground motion fields

The generation of spatially correlated ground motion fields is based on the work of Jayaram and Baker [2009] where they propose a model - based on a semivarigram - for describing

$$\gamma(h) = a\left[1 - \exp\left(-\frac{3h}{b}\right)\right] \tag{7.1}$$

7.3. Stochastic PSHA calculator

The OpeQuake stochastic PSHA calculator provides a way to check the consistency between the result provided by a classical PSHA calculator and the results that can be obtained by a number of ground motion fields, representative of the

CHAPTER 8

Wesson et al. [2009] risk calculation implementation

In the procedure proposed by Wesson et al. [2009] the creation of the ERF follows the classical approach.

Using an ERF, for each rupture Rup is possible to calculate the probability that a given ground motion U is in the interval $u_x \pm \Delta u$ given an inter-event variability ϵ_{inter} (this corresponds to equation 3 of Wesson et al. [2009]):

$$\begin{aligned} P(u_x - \Delta u \leq U < u_x + \Delta u | Rup, \epsilon_{inter}) &= \Phi\left(\frac{\ln(u_x - \Delta u) - \ln(u_0)}{\sigma_{intra}}\right) - \\ &- \Phi\left(\frac{\ln(u_x + \Delta u) - \ln(u_0)}{\sigma_{intra}}\right) \end{aligned} \tag{8.1}$$

where $\ln(u_0)$ is the mean of the GMPE computed considering a value ϵ_{intra} and a rupture Rup, (generally characterized by a geometry and a magnitude) and Φ is the standard normal CDF.

The next step is to calculate the PMF of losses for a given rupture. Given an asset, the probability of suffering a loss value in the interval $[l - \Delta l, l + \Delta[$ given a ground motion value in the interval $[u_x - \Delta u, u_x + \Delta u[$ (note that in this case the distribution of ground motion u will depend on ϵ_{intra}) corresponds to:

$$\begin{aligned} P(l - \Delta l \leq L < \; & l - \Delta l | Rup, \epsilon_{inter}) = \\ \sum_{x=0}^{\infty} \; & P(l - \Delta l \leq L < l - \Delta l | u_x + \Delta u \leq U < u_x + \Delta u) \\ & P(u_x - \Delta u \leq U < u_x + \Delta u | R, \epsilon_{inter})) \end{aligned} \tag{8.2}$$

If $P^i(L = l | Rup, \epsilon_{inter})$ corresponds to the conditional probability mass function describing the discrete probability of having a loss in the interval $[l - \Delta l, l - \Delta[$ for the asset with index i, the probability of cumulated losses to a portfolio can be computed as:

$$P_{CL}(CL = cl|M, \epsilon_{inter}) = P^1(L = l|Rup, \epsilon_{inter}) * \ldots * P^n(L = l|Rup, \epsilon_{inter}) \quad (8.3)$$

where symbol $*$ stands for convolution.

Finally, the total probability of exceeding a given level of cumulated losses cl computed considering the contributions of all the ruptures occurring on all the seismic sources considered is (note that this expression extends equation A10 of Field et al. [2003]):

$$P(CL \geq cl) = 1 - \prod_{i=1}^{n} \left(1 - \sum_{n=1}^{N(i)} \sum_{k=-3}^{3} P(Rup_{i,n}) P(CL \geq cl|Rup_{i,n}, \epsilon_k) \right) \quad (8.4)$$

where $P(CL \geq cl|Rup_{i,n}, \epsilon_k)$ can be simply derived from the PMF $P_{CL}(CL = cl|M, \epsilon_{inter})$, n is the number of seismic sources.

PART III

Risk

CHAPTER 9

OpenQuake Input Description: Risk

The two main sources of input information required for a risk calculation with OpenQuake are an exposure model and a vulnerability model (in addition to the calculation type, such as those described in the subsequent chapters, and the region of interest). An exposure model for a given asset category describes, at each location of interest within a given region, the value of each asset typology. The vulnerability model describes the vulnerability characteristics of each asset typology.

9.1. Exposure

The OpenQuake engine requires an exposure model that needs to be stored according to the respective NRML schema. This file format can include several typologies of asset such as population or buildings. The following parameters are currently being used to describe each asset of the exposure model:

- Asset ID: A unique key used to identify the asset instance;
- Asset description: Brief description of the asset typology;
- Asset value: Numerical value of the quantity of the asset;
- Location: Geographic coordinates of the asset expressed in decimal degrees.

This list of parameters will be further extended in future releases of OpenQuake once more complex data will need to be stored (e.g. value of contents or number of occupants per building at different times of the day).

9.2. Vulnerability

Vulnerability is defined as the probability distribution of loss, given an intensity measure level. Vulnerability functions can be derived directly, usually through empirical methods where the losses from past events at given locations are related to the levels of intensity of ground motion at those locations, or they can be derived by combining fragility functions and consequence functions. Fragility functions describe the probability of exceeding a set of limit states, given an intensity measure level; limit states describe the limits to performance levels, such as damage or injury levels. Fragility functions can be derived by expert-opinion, empirically (using observed data), or analytically, by explicitly modeling the behavior of a given asset typology when subjected to increasing levels of ground motion. Consequence functions describe the probability distribution of loss, given a performance level and are generally derived empirically. Version 0.2 of OpenQuake only supports vulnerability functions. However, the possibility to describe the vulnerability characteristics of the exposed assets with fragility and consequence functions is planned in future releases of OpenQuake such that users can view intermediate results of seismic loss calculations, such as the distribution of damage or injury levels.

9.2.1. Vulnerability Function

9.2.1.1. Discrete Vulnerability Functions

In the current version of OpenQuake (V0.2) discrete vulnerability functions are used to directly estimate human and economic losses. Discrete vulnerability functions are described by a list of intensity measure levels and corresponding mean loss ratios (the ratio of mean loss to exposed value), associated coefficients of variation and probability distributions. The uncertainty on the loss ratio is assumed in OpenQuake v0.2 to follow a lognormal distribution, however different probabilistic distributions for the uncertainty will be developed in future versions such as the beta distribution. Figure 9.1 illustrates a discrete vulnerability function.

9.2.1.2. Continuous Vulnerability Functions

In version 0.3 of OpenQuake, continuous vulnerability functions will be implemented. Continuous vulnerability functions are described by continuous distributions of mean loss ratio and coefficient of variation with ground motion intensity. Figure 9.2 illustrates this type of function.

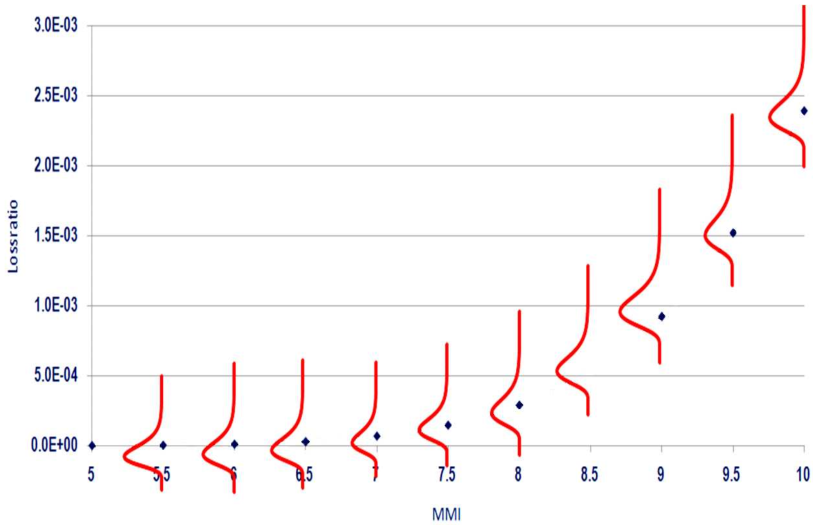

Figure 9.1.: Discrete vulnerability function.

9.2.2. Fragility Functions

Fragility functions describe the probability of exceeding a set of limit states, given an intensity measure level. When the asset category concerns structures (e.g. buildings), the intensity measure can either be structure-independent or structure-dependent. The former can be calculated directly from recorded measurements of ground shaking (e.g. peak ground acceleration, peak ground velocity, spectral acceleration at a given period of vibration, or even macroseismic intensity). The latter requires information on the characteristics of the structures in order to be calculated, for example spectral acceleration at the fundamental period of vibration, or spectral displacement at the limit state period of vibration. The calculation of these structural characteristics might be through a simple formula (e.g. a yield period-height equation, see e.g. Crowley and Pinho [2004]) or through so-called non-linear static methods, which are needed when the intensity measure is a non-linear response quantity such as spectral displacement at the limit state period of vibration (see e.g. FEMA-440:ATC [2005]). Discrete and continuous fragility functions with structure-independent intensity measures aim to be implemented in version 0.3 of OpenQuake. Fragility functions with structure-dependent intensity measures (and the methods necessary to calculate them) will be planned for the version 0.5 release.

9.2.2.1. Discrete Fragility Functions

Fragility functions can be defined in a discrete way by providing for each limit state a list of intensity measure levels and respective probabilities of exceedance. Figure 9.3

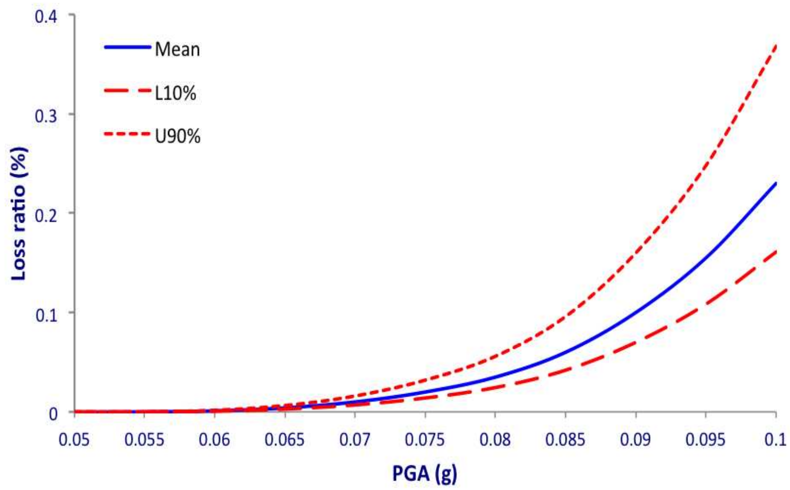

Figure 9.2.: Continuous vulnerability function.

presents a set of discrete fragility functions using a macroseismic intensity measure.

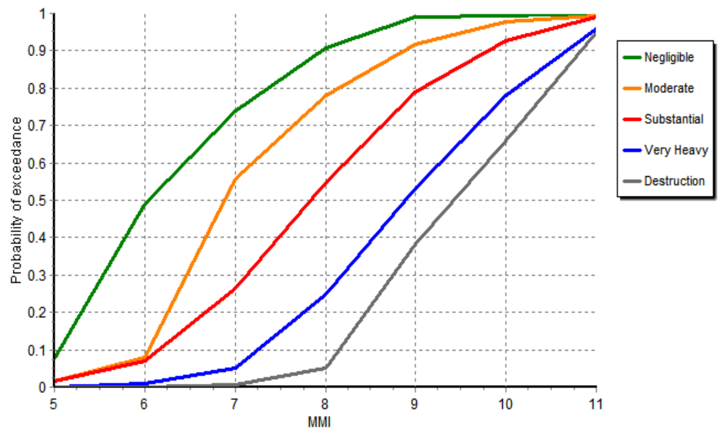

Figure 9.3.: Set of discrete fragility function.

9.2.2.2. Continuous Fragility Functions

Continuous fragility functions are defined by the parameters of a cumulative distribution function. In Figure 9.4 an example of a set of continuous fragility functions with a structure-dependent intensity measure is presented.

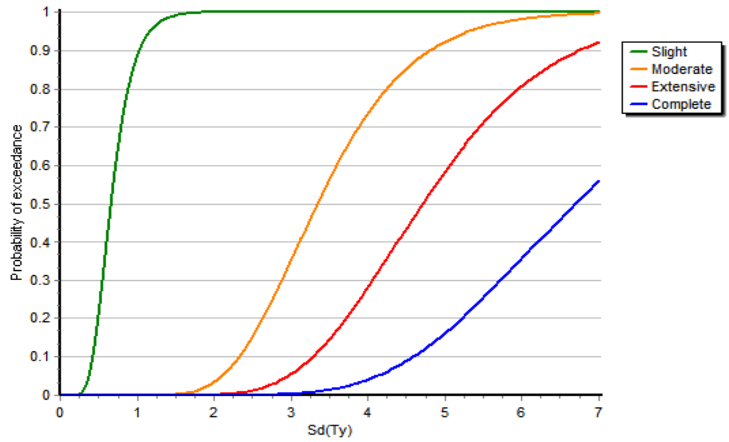

Figure 9.4.: Set of continuous fragility function.

9.2.3. Consequence Functions

Consequence functions describe the probability distribution of loss, given a performance level. For example, if the asset category is buildings and the performance level is significant damage, the consequence function will describe the mean loss ratio, coefficient of variation and probability distribution for that level of damage. Figure 9.5 presents the mean damage ratio for a set of performance levels proposed by two different sources:

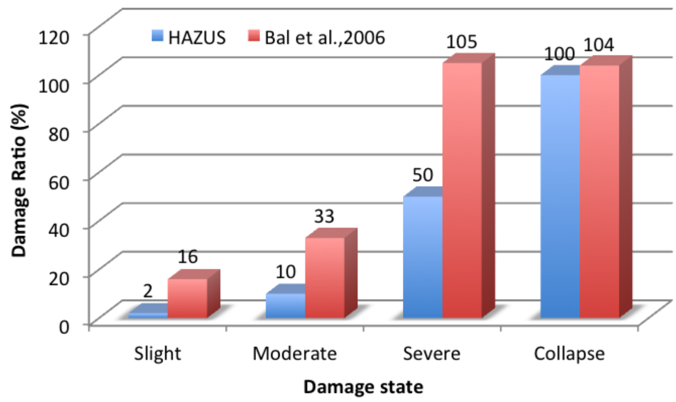

Figure 9.5.: Consequence functions adapted from Bal et al. [2010]

CHAPTER 10

Deterministic event based calculator

The deterministic event-based calculator is capable of computing losses and loss statistics for a single event for a collection of assets. Depending of the type of hazard input that is provided, two separate approaches can be followed. In the first one, the calculator uses two maps, one with the distribution of the mean ground motion and a second one with the associated aleatory variability. In the second approach, the event is repeated many times to model the variation in the inter-event variability and for each event, a ground motion field is generated taking into account the intra-event variability (and possibly the spatial correlation of the latter). Figure 10.1 presents the architecture of this calculator:

10.1. Method A

10.1.1. Description

In this approach, after providing the two aforementioned maps, the mean ground motion and coefficient of variation at each site are used together with the assigned vulnerability function for each asset to calculate a mean loss ratio. The aleatory variability in the ground motion is combined with the uncertainty in the vulnerability functions through the total probability theorem in order to calculate the standard deviation of the loss ratio for each asset.

10.1.2. Calculation workflow

To compute the mean loss:

1. In order to compute the probability of occurrence of each intensity measure level defined on the vulnerability function, an upper and lower bound needs to be

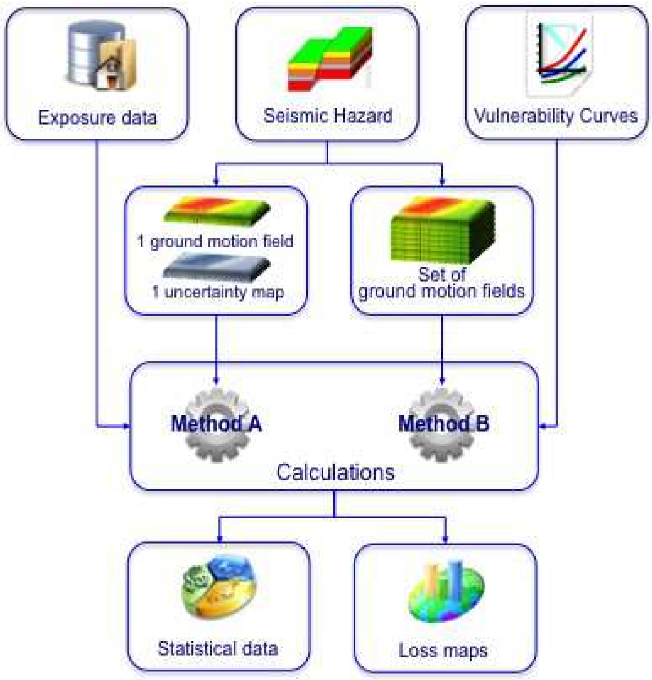

Figure 10.1.: Architecture of the deterministic event-based calculator.

calculated for each value. The limits for an IML_n can be given by the following formulae:

$$Lowerbound = \frac{IML_n + IML_{n-1}}{2} \tag{10.1}$$

$$Upperbound = \frac{IML_{n+1} + IML_n}{2} \tag{10.2}$$

Figure 10.2 illustrates the intervals that were computed based on 4 intensity measure levels that comprise a given vulnerability function:

Note that for the first and last intensity measure level, there are no values before or after respectively. In this case, the lower and upper bound need to be computed based on the distance between the respective intensity measure level and the bound that was computed through one of the aforementioned formulae. Thus, the lower bound for the first intensity measure level can be given by:

$$Lowerbound[IML_1] = IML_1 - \frac{IML_2 - IML_1}{2} \tag{10.3}$$

And the upper bound for the last intensity measure level can be computed using:

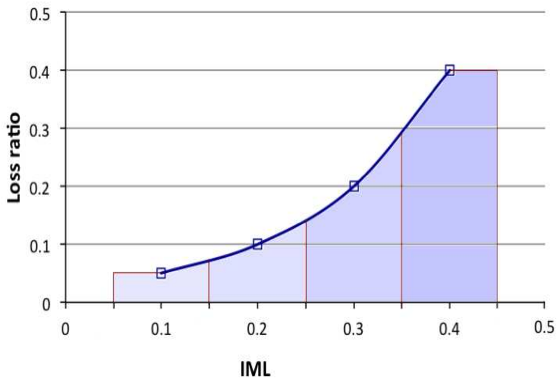

Figure 10.2.: Intervals for each intensity measure level on a discrete vulnerability function.

$$Upperbound[IML_n] = IML_n + \frac{IML_n - IML_{n-1}}{2} \tag{10.4}$$

2. Once the intervals for each intensity measure level are defined, the probability of occurrence can be computed through the expression:

$$PO[IML_n] = F(UB, \mu, \sigma) - F(LB, \mu, \sigma) \tag{10.5}$$

Where F stands for the cumulative distribution function, UB and LB stand for the upper and lower bound respectively of the IML_n and μ and σ stand for the logarithmic mean and standard deviation i.e. the mean ground motion and associated standard deviation of the normal distribution of the natural logarithm of the ground motion values.

3. Then, the mean loss ratio for each asset can be computed through the formula:

$$LR = \sum_{n=1}^{m} PO[IML_n] \times LR_n \tag{10.6}$$

4. The absolute mean loss can be computed by multiplying the mean loss ratio by the value of the asset contained on the exposure model file.

To compute the standard deviation of the loss:

1. In order to compute this parameter, the total probability theorem needs to be used. The first step is to compute $E[LR_n^2]$, which is given by the following formula:

$$E[LR_n^2] = SD[LR_n]^2 + E[LR_n]^2 \quad (10.7)$$

Where $SD[LR_n]$ stands for the standard deviation of the distribution of loss ratios and $E[LR_n]$ stands for the mean loss ratio.

2. Then, the total $E[LR^2]$ can be derived using the formula:

$$E[LR^2] = \sum_{n=1}^{m} PO[IML_n] \times E[LR_n]^2 \quad (10.8)$$

3. Subsequently the standard deviation of the loss ratio can be computed using the expression:

$$SD[LR] = \sqrt{E[LR^2] - E[LR]^2} \quad (10.9)$$

Where $E[LR]$ stands for the mean loss ratio computed previously.

4. The absolute standard deviation of the loss can finally be computed by multiplying the standard deviation of the loss ratio by the value of the respective asset.

10.2. Method B

10.2.1. Description

In this approach, for each ground motion field, the intensity measure level at a given site is combined with a vulnerability function to randomly sample a loss ratio for each asset typology defined in the exposure file. contained in the exposure model. These loss ratios that are sampled for a given typology at different locations are considered to be independent or fully correlated, knowing that the reality is likely to lie somewhere in between these two assumptions. Using these results, the mean and standard deviation of loss ratio across all events can be calculated. Again, loss ratios are converted into losses by multiplying by the value of the asset given in the exposure file. For this method, it is possible to aggregate the losses throughout the region and to compute the standard deviation of the aggregated loss.

10.2.2. Calculation workflow

To compute the mean loss:

1. For each ground motion field, the intensity measure level at the location of the asset is used to derived the mean loss ratio and associated coefficient of variation from the vulnerability function. Since currently the vulnerability functions are being defined in a discrete way, it is quite probable that the intensity measure level provided by the ground motion field is not contained in the vulnerability function. In these cases, linear interpolation methods are being employed to derive the mean loss ratio at the intensity measure level of interest. Once these two parameters are known, the sampling of the loss ratio is done following the probabilistic distribution of the respective vulnerability function, as described bellow:

$$\log LR_n = \mu + \epsilon\sigma \tag{10.10}$$

   Where μ and σ stand for the mean and standard deviation of the logarithm of the loss ratios respectively and ϵ is a term that has a standard normal distribution with a zero mean and a standard deviation of one.

   The method used to sample this parameter can follow two approaches depending on whether the correlation between the vulnerability of similar asset typologies is to be considered or not:

   - Perfectly correlated: the term ϵ is randomly sampled once for the first asset and this result is used to derive the loss ratio for all the assets of the same typology.
   - Uncorrelated: the term ϵ is always randomly sampled for each asset and therefore the correlation between the vulnerability of the assets is ignored.

   It is expected that the true level of correlation lies somewhere between these two assumptions, and thus they provide boundaries to the expected output.

2. The mean loss ratio for each asset across all possible simulations of the deterministic event can be calculated through the formula:

$$LR = \frac{\sum_{n=1}^{m} LR_n|IML}{m} \tag{10.11}$$

   Where m stands for the number of ground motion fields simulated.

3. The mean loss can then be derived by multiplying the mean loss ratio by the value of the asset contained in the exposure model file.

To compute the standard deviation of the loss:

1. In order to compute the uncertainty, the engine takes the set of loss ratios for each asset, and computes the associated standard deviation using the classical formula:

$$SD[LR] = \sqrt{\frac{1}{m}\sum_{n=1}^{m}(LR_n - E[LR])^2} \tag{10.12}$$

   Where $E[LR]$ stands for the mean loss ratio computed previously.

2. The standard deviation of the absolute loss can finally be computed by multiplying the standard deviation of the loss ratio by the value of the respective asset.

CHAPTER 11

Classical PSHA-based calculator

11.1. Description

The Classical PSHA-based risk calculator can be used to determine loss exceedance curves under certain conditions (usually for single site loss assessments). This calculator takes the configuration information, one or several vulnerability models, information describing the assets and using hazard curves, either contained in a file or computed using a PSHA input model, computes a loss exceedance curve for each asset. Figure 11.1 illustrates the architecture of this calculator:

11.2. Calculation workflow

1. By default, the hazard component of the OpenQuake engine computes the hazard curves for a set of intensity measure levels that are pre-defined in the configuration file. With the integration of the hazard and risk components in the engine, a feature is currently being implemented with the purpose of verifying that this set of values covers the range of intensity measure levels defined in the vulnerability functions. If not, the set of values in which the hazard curves are going to be computed is extended based on the minimum and maximum values of the vulnerability functions.

2. To use this calculator (to be released with V0.3), the hazard curves need first to be converted into probability mass functions (e.g. probability of occurrence of a discrete set of intensity measure levels). To do so, the engine starts by reading the intensity measure levels from the discrete vulnerability functions, and computes the central value between consecutive levels. Two consecutive values define the boundaries of the interval for each intensity measure level and by relating these limits with the hazard curve, the engine computes the corresponding probabilities

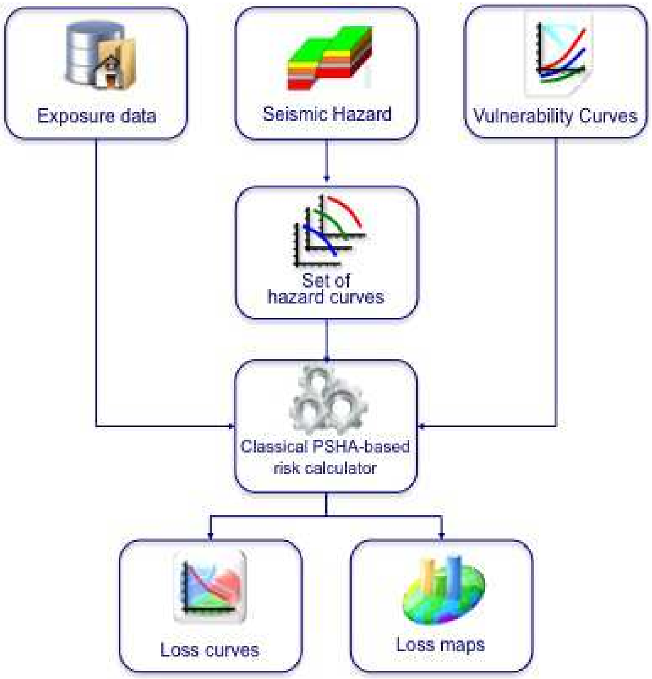

Figure 11.1.: Architecture of the Classical PSHA-based risk calculator.

of exceedance. Figure 11.2 contains a discrete vulnerability function (bottom chart) and a hazard curve (top chart) in which the definition of the interval for a given intensity measure level and associated estimation of the probabilities of exceedance of each limit are illustrated.

3. The probability of occurrence of the intensity measure levels that fall within each interval can be derived by subtracting the probabilities of exceedance of the lower and upper limits, as described by the following formula:

$$PO = PE[lowerbound] - PE[upperbound] \tag{11.1}$$

4. The discrete vulnerability functions for each asset are converted into loss ratio exceedance matrices (e.g. matrices which describe the probability of exceedance of each loss ratio for a discrete set of intensity measure levels). These matrices have a number of columns equal to the number of intensity measure levels defined on the vulnerability function and a number of rows that can go from the number of loss ratios defined by the discrete function, up to any multiple of this number. In order to properly incorporate the probabilistic distribution of loss ratios per intensity measure level, the probabilities of exceedance should be computed not just for the loss ratios defined on the vulnerability function, but

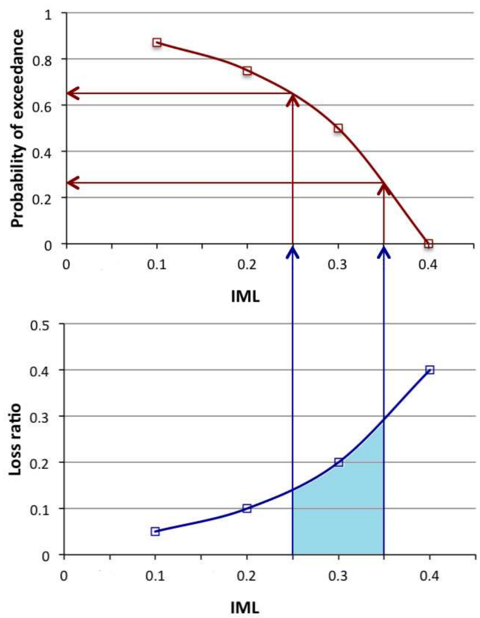

Figure 11.2.: Workflow to estimate the probabilities of exceedance of the boundaries of each intensity measure level.

also for many intermediate values between consecutive loss ratios. Currently, following a number of sensitivity analyses, the OpenQuake engine considers 5 intermediate values between consecutive loss ratios, however, this is a parameter that will be adjustable by the user. Figure **??** contains an example of a discrete vulnerability function and the respective loss ratio exceedance matrix (in light gray):

Note that for this example only one intermediate value was considered between consecutive loss ratios and in order to consider the whole distribution of the loss ratios, the matrix was computed considering a minimum and maximum loss ratio of 0 and 1 respectively.

5. Finally, each column of the aforementioned matrix is multiplied by the probability of occurrence of the respective intensity measure level (extracted from the hazard curves) to produce a conditional loss ratio exceedance matrix. Then, for each loss ratio the probabilities of exceedance are summed, leading to a loss ratio exceedance curve, whose set of loss ratios can be multiplied by the value of the asset given by the exposure file to obtain an absolute loss exceedance curve.

IML	LR	COV
0.1	0.05	0.5
0.2	0.08	0.3
0.4	0.20	0.2
0.6	0.40	0.1

	0.1	0.2	0.4	0.6
0.00	1.00	1.00	1.00	1.00
0.03	0.89	1.00	1.00	1.00
0.05	0.41	0.93	1.00	1.00
0.07	0.21	0.71	1.00	1.00
0.08	0.11	0.44	1.00	1.00
0.14	0.01	0.02	0.96	1.00
0.20	0.00	0.00	0.46	1.00
0.30	0.00	0.00	0.02	1.00
0.40	0.00	0.00	0.00	0.48
0.70	0.00	0.00	0.00	0.00
1.00	0.00	0.00	0.00	0.00

Figure 11.3.: Example of a discrete vulnerability function and respective loss ratio exceedance matrix.

CHAPTER 12

Probabilistic event-based calculator

12.1. Description

This method uses stochastic event sets and associated ground motion fields to compute loss curves for each asset contained in an exposure file, as illustrated in Figure 12.1 :

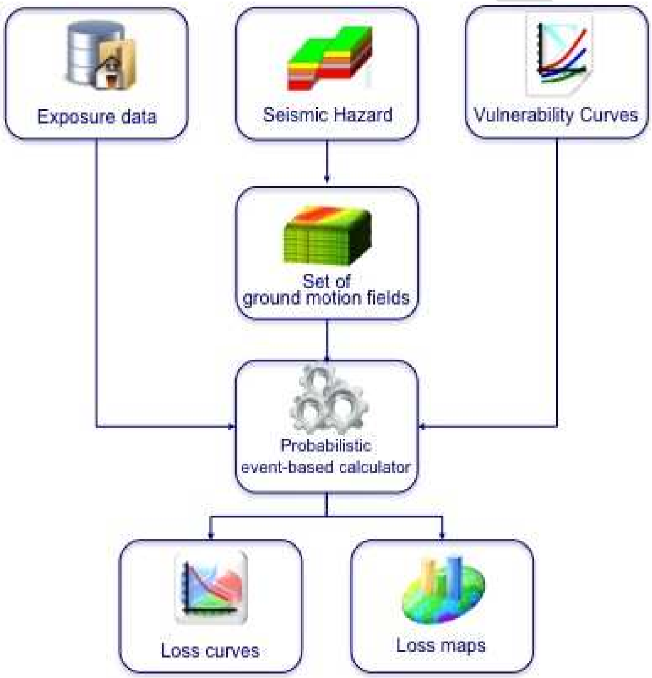

Figure 12.1.: Architecture of the probabilistic event-based calculator.

For each ground motion field, the intensity measure level at a given site is used along with the vulnerability function to randomly sample the loss ratio for each asset typology defined in the exposure file. The loss ratios that are sampled for a given typology at different locations in the exposure model are considered to be independent or fully correlated, knowing that the reality is likely to lie somewhere in between these two assumptions. The occurrence distribution of mean loss for a given asset is calculated using all of the ground motion fields, leading to a histogram of loss ratios which is then converted into a cumulative histogram, by calculating the number of cumulative occurrences for each interval of loss ratio. The rate of exceedance of each loss ratio is calculated by dividing the number of cumulative occurrences by the number of stochastic event sets multiplied by the length of each event set. By assuming a Poissionian distribution of the occurrence model, the probability of exceedance of each loss ratio is calculated.

If an aggregated loss curve for a portfolio of assets is required, a secondary module is necessary in order to aggregate the losses from all the assets in the exposure file, per event, before calculating the occurrence distribution of mean loss. If the assets are close enough, it is necessary to generate the ground motion fields taking into account the spatial correlation of ground motion residuals.

12.2. Calculation workflow

1. The engine starts by using the set of ground motion fields to extract the intensity measure levels for the location of each asset.

2. Then the engine takes the vulnerability function assigned to each asset and checks if the uncertainty was specified. If not, the loss ratios are derived based on the mean loss ratio for each intensity measure level. However, if the uncertainty is defined, it is randomly sampled following the probabilistic distribution, mean loss ratio and associated coefficient of variation of the respective function, as described bellow:

$$\log LR_n = \mu + \epsilon\sigma \tag{12.1}$$

Where μ and σ stand for the mean and standard deviation of the logarithm of the loss ratios respectively and ϵ is a term that has a standard normal distribution with a zero mean and a standard deviation of one.

The method used to sample this parameter can follow two approaches depending on whether the correlation between the vulnerability of similar asset typologies is to be considered or not:

- Perfectly correlated: the term ϵ is randomly sampled once for the first asset and this result is used to derive the loss ratio for all the assets of the same typology.
- Uncorrelated: the term ϵ is always randomly sampled for each asset and therefore the correlation between the vulnerability of the assets is ignored.

It is expected that the true level of correlation lies somewhere between these two assumptions, and thus they provide boundaries to the expected output.

3. In this method a histogram of the loss ratios per asset is required. Before the histogram can be built, it is necessary to define the number and width of the bins. The former might vary significantly since it might depend of several factors (e.g. number of ground motion fields, range of ground motion covered by the vulnerability model) while the later is related with the minimum and maximum values of loss ratio previously computed and with the number of bins.

4. The histograms for each asset need to be converted into a cumulative histogram. The number of occurrences for each bin can be derived using the following formula:

$$NCO_m = \sum_{n=m} NO_n \tag{12.2}$$

where NCO_m stands for the number of cumulative occurrences of the m^{th} bin of the cumulative histogram and NO_n stands for the number of occurrences of the n^{th} bin of the histogram of the loss ratios.

5. Thereafter, the rate of exceedance of a set of loss ratios needs to be computed for each asset. This set of loss ratios is comprised of the middle values of each bin of the cumulative histogram. The following formula is employed to compute this rate:

$$\lambda(LR_n) = \frac{NCO_n}{TSES} \tag{12.3}$$

Where λ stands for the rate of exceedance of the respective loss ratio and $TSES$ stands for the time representative of all stochastic event sets which means, the number of stochastic event sets multiplied by the time span of each.

6. Assuming a Poissonion distribution of the occurrence model, the probability of exceedance of the set of loss ratios can be derived using the following formula:

$$PE(LR_n) = 1 - \exp -\lambda_n \times t \tag{12.4}$$

Where t stands for the time span used to produce the stochastic event set.

CHAPTER 13

Displacement-Based Earthquake Loss Assessment

13.1. Description

The DBELA methodology is a nonlinear static analytical for the seismic risk assessment of buildings. This method arises as a solution to the lack of a methodology capable of combining good correlation with damage, easy to calibrate, transparent, theoretically robust and with a full probabilistic treatment of the variables. As a continuation of the urban assessment methodology proposed by Calvi [1999] in which principals of structural mechanics and seismic response of buildings are used to estimate the seismic vulnerability of classes of buildings, Pinho et al. [2002] presents for the first time a displacement-based earthquake loss assessment methodology. Glaister and Pinho [2003] carried out further developments on the equations and Crowley et al. [2004] adapted the methodology to assess RC buildings in a more practical way. The introduction of a probabilistic framework capable of considering the uncertainty on the demand and capacity was proposed by Crowley et al. [2006] and in [Bal et al., 2010] new contributions were added to the methods such as the inclusion of new failure mechanisms and building typologies or the evaluation and quantification of the uncertainty of several parameters. The most up to date version of this methodology is described herein highlighting the building typologies that can be considered, the formulas that are being employed and how the uncertainty is being taking into account.

13.2. Procedure

This methodology is strongly based on the Displacement-based Design rules introduced by Priestley [1997] and Priestley et al. [2007] in which a multiple degree of freedom

(MDOF) structure is converted in to an equivalent structure with a single degree of freedom (SDOF). Then, the following parameters need to be computed:

- Limit state displacement capacity;
- Limit state ductility values;
- Limit state periods;
- Displacement demand;

Once these parameters are obtained, the displacement capacity of the first limit state is compared with the respective demand. If the demand exceeds the capacity, the next limit states need to be checked successively, until the demand no longer exceeds the capacity and the building damage state can be defined. If the demand also exceeds the last limit state, the building is assumed to have collapsed. This procedure can be schematically seen in Figure 13.1 in which the capacity for each limit state is being represented by Δ_{LS} and the associated demand by S_{di}. In this example, the demand exceeds the capacity in first and second limit state but not on the third limit state which allocates the building in the third damage state.

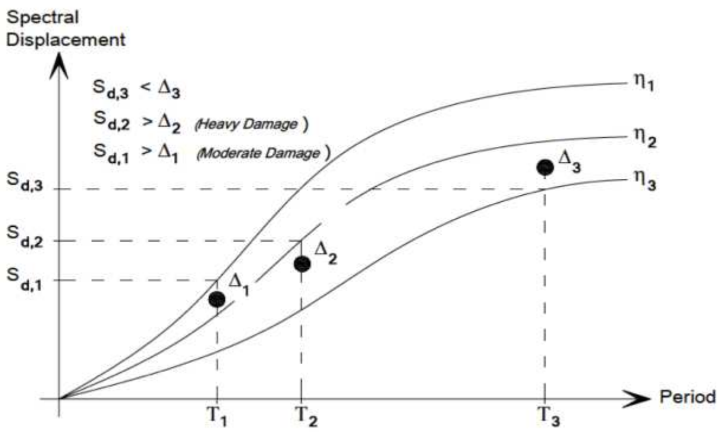

Figure 13.1.: Comparison between the capacity for each limit state and the associated demand [Bal et al., 2010].

Each displacement capacity (Δ_{LS}) is computed based on the secant stiffness at the respective limit state and a level of equivalent viscous damping, representative of the combined elastic damping and hysteretic energy absorbed during the inelastic response [Bal et al., 2010]. The respective displacement demand can either be calculated using an over-damped spectrum or using a ground motion prediction equation (GMPE). In both cases, the displacement demand is computed for the period at each limit state and modified by a correction factor η_i, representative of the equivalent viscous damping and limit state ductility. The formulas that are employed to compute the previously described parameters can vary based on the type of structure. The following section presents the most of to date equations for each building typology currently covered by the methodology.

13.3. Building typologies

The building typologies that can be assess through this method were grouped into Reinforced Concrete and Masonry structures. A description of the whole displacement-based procedure for each building typology can be found in [Bal et al., 2010]. For what concerns this document, it will be presented the most important formulas and parameters. The following list describes the symbols that will be used on the aforementioned formulas:

Table 13.1.: Summary of the symbols

Symbol	Description
Δ_{Sy}	Limit state 1 (yield) structural displacement capacity
Δ_{SLSi}	Limit state i (post-yield) structural displacement capacity
ef_h	Effective height coefficient
ϵ_y	Yield strain of reinforcement steel
$\epsilon_{C(LS_i)}$	Limit state i (post-yield, spalling/crushing) concrete strain
$\epsilon_{S(LS_i)}$	Limit state i (post-yield) reinforcement steel strain
h_c	Depth of column section
h_s	Height of ground-floor storey
h_b	Height of beam
l_b	Length of beam
T_y	Yield period of vibration
T_{LS_i}	Limit state i (post-yield) period of vibration

13.3.1. Reinforced Concrete Buildings

13.3.1.1. Frames with emergent or embedded beams

A great proportion of the residential and commercial Mediterranean buildings are constructed in reinforced concrete with masonry infills. Such buildings tend to have a beam-column frame structural behavior in which the masonry panels might not have a robust connection to the frame. These structures can either follow a joist-slab-column system in which the slabs are built between embedded beams with a thin layer of concrete on the top of the hollow bricks (embedded beams), or another construction typology in which the beams depth are considerably greater than the slab depth (emergent bems). In the first construction approach the columns tend to be larger due to the fact that the distribution of the moments around the joint required the column to withstand higher levels of stress [Bal et al., 2010]. In Figures 13.2 and 13.3 the differences between these two types of construction can be seen.

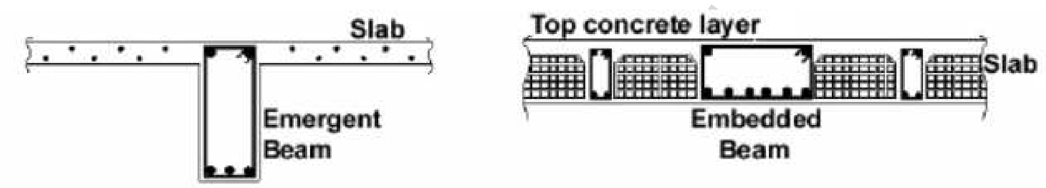

Figure 13.2.: Cross section of emergent beam (left) and embedded beam (right)[Bal et al., 2010].

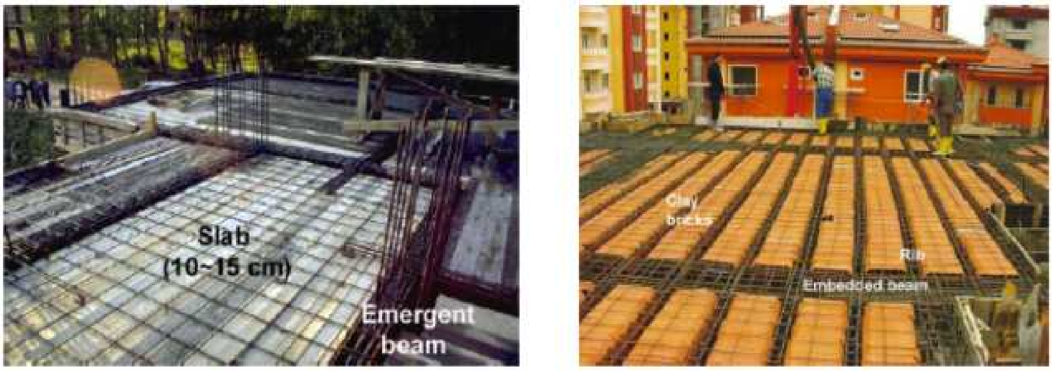

Figure 13.3.: Construction application of emergent beam (left) and embedded beam (right)[Bal et al., 2010].

Bare frame structures

The procedure proposed by [Crowley et al., 2006] for bare frames have been used, with the exception of the equations to estimate the deformed shape that were replaced by the ones presented by [Priestley et al., 2007]. The displacement capacity and ductility values for each limit state depend on the failure mechanism that will affect the structure. Two response mechanisms are considered within the methodology: beam-sway and column-sway, as described by Paulay and Priestley [1992]. Thus, to compute the yield (first limit state) displacement capacity for beam-sway and column-sway bare frames, the following formulae can be used respectively:

$$\Delta_{Sy} = 0.50\delta_{eff} H_T \epsilon_y \frac{l_b}{h_b} \tag{13.1}$$

$$\Delta_{Sy} = 0.43\delta_{eff} H_T \epsilon_y \frac{h_s}{h_c} \tag{13.2}$$

The post-yield displacement capacity for the second and third limit state are calculated by adding a plastic displacement component to the yield displacement, obtaining the following formulae:

$$\Delta_{Sy} = 0.50\delta_{eff} H_T \epsilon_y \frac{l_b}{h_b} + 0.5(\epsilon_{C(LS_i)} + \epsilon_{S(LS_i)} - 1.7\epsilon_y)\delta_{eff} HT \tag{13.3}$$

$$\Delta_{Sy} = 0.43\delta_{eff} H_T \epsilon_y \frac{l_b}{h_b} + 0.5(\epsilon_{C(LS_i)} + \epsilon_{S(LS_i)} - 2.14\epsilon_y) h_s \tag{13.4}$$

The effective height coefficient δ_{eff} in the above formulae can be compute for beam-sway frames using equations:

$$for \quad n \leq 4 \quad \delta_{eff} = H_i / H_T \tag{13.5}$$

and

$$for \quad n > 4 \quad \delta_{eff} = (4/3)(H_i/H_T)(1 - H_i/(4H_T)) \tag{13.6}$$

Where H_i stands for the height of the storey, H_T stands for the total height of the building and n stands for the number of storeys. Regarding column-sway frames, the equation first proposed by Priestley [1997] and then adapted by Glaister and Pinho [2003] can be used:

$$\delta_{eff} = 0.67 - 0.17 \frac{\mu_{LSi} - 1}{\mu_{LSi}} \tag{13.7}$$

It should be noted that the ductility values μ_{LSi} for column-sway frames also depend on the δ_{eff} as it will be shown ahead. In this case, an iterative procedure needs to be employed. However, in order to overcome this issue, Glaister and Pinho [2003] proposed a similar formula in which the ductility was replaced by the steel strain:

$$\delta_{eff} = 0.67 - 0.17 \frac{\epsilon_{LSi} - \epsilon_y}{\epsilon_{LSi}} \tag{13.8}$$

Within OpenQuake, both approaches have been implemented and users can choose which one should be followed. Each limit state ductility value μ_{LSi} for beam-sway and column-sway frames can be obtained by dividing the displacement capacity of the respective limit state by the yield displacement capacity, as shown respectively in the following equations:

$$\mu_{LSi} = 1 + \frac{(\epsilon_{C(LS_i)} + \epsilon_{S(LS_i)} - 1.7\epsilon_y)h_b}{\epsilon_y l_b} \tag{13.9}$$

$$\mu_{LSi} = 1 + \frac{(\epsilon_{C(LS_i)} + \epsilon_{S(LS_i)} - 2.14\epsilon_y)h_c}{0.86\delta_{eff} H_T \epsilon_y} \tag{13.10}$$

Regarding the period for each limit state, different equations have been proposed for bare frames with emergent beams or embedded beam. For the former, Crowley and Pinho [2004] suggested a yield period equal to $0.1H_T$ while for the later, as presented by Kumar [2008] and verified by Bal et al. [2010], a yield period equal to $0.12H_T$ can be assumed. As for the second and third limit state period, if the post-yield stiffness ratio can be neglected, the following formula proposed by Crowley et al. [2006] can be employed:

$$T_{LS} = T_y \sqrt{\mu_{LS}} \tag{13.11}$$

Infilled frame structures

The presence of masonry infill walls increases the strength of the building and slightly decreases the displacement capacity. In order to incorporate the decrease on the displacement capacity on the respective equations, a parameter β_i which varies between 0 and 1 has been added to the formulae used for bare frame structures. Thus, the following equations for beam-sway and column-sway can be used respectively:

$$\Delta_{Sy} = \left[0.50\delta_{eff} H_T \epsilon_y \frac{l_b}{h_b}\right] \beta_1 + \left[0.5(\epsilon_{C(LS_i)} + \epsilon_{S(LS_i)} - 1.7\epsilon_y)\delta_{eff} H_T\right] \beta_2 \tag{13.12}$$

$$\Delta_{Sy} = \left[0.43\delta_{eff} H_T \epsilon_y \frac{l_b}{h_b}\right] \beta_1 + \left[0.5(\epsilon_{C(LS_i)} + \epsilon_{S(LS_i)} - 2.14\epsilon_y)h_s\right] \beta_2 \tag{13.13}$$

Bal et al. [2010] ran several displacement-based adaptive pushover analysis on a set of mediterranean buildings with the purpose of evaluating the decrease on the displacement capacity for each limit state. Using these results, a mean β_i have been proposed as given in Table 13.2.

As far as period-height relationship, the increase in strength causes a decreases on the yield period. For emergent beam infilled frames, Crowley and Pinho [2006] suggested a yield period equal to $0.055H_T$ while for embedded beam infilled frames, Kumar [2008] proposed a yield period equal to $0.06H_T$. Regarding the post-yield periods, the same procedure suggested for bare frame structures can be employed (see equation 13.11).

Table 13.2.: Mean β_i values

Infilled Case	$LS1(\beta_1)$	$LS2(\beta_2)$	$LS3(\beta_2)$
Embedded beam frames	0.60	0.62	0.49
Emergent beam frames	0.52	0.46	0.28

13.3.1.2. Frame-wall structures

Often buildings have both frames and walls contributing to the seismic resistance, as illustrated in Figures 13.4 and 13.5.

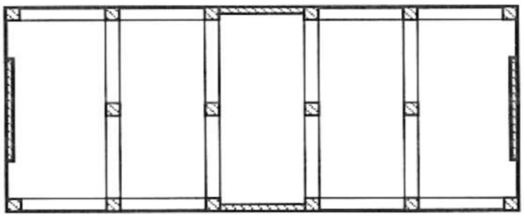

Figure 13.4.: Plan view of a dual wall-frame structure [Priestley et al., 2007].

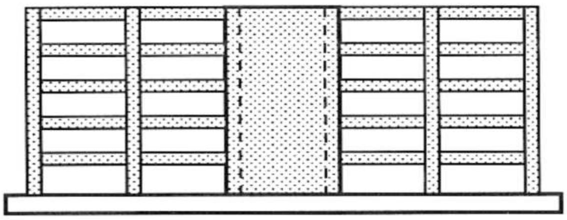

Figure 13.5.: Front view of a dual wall-frame structure [Priestley et al., 2007].

As far as the DBELA methodology concerns, the procedure defined by Sullivan et al. [2006] and Priestley et al. [2007] was adopted. Thus, assuming that a shear-away failure mechanism is not likely to occur, the displacement capacity can be given by the following formulae:

$$for \quad H_i \leq H_{CF} \quad \Delta_{yi} = 2\epsilon_y/l_w(H_i^2/2 - H_i^3/(6H_{CF})) \tag{13.14}$$

$$for \quad H_i \geq H_{CF} \quad \Delta_{yi} = 2\epsilon_y/l_w(H_{CF}H_i/2 - H_{CF}^2/6)) \tag{13.15}$$

$$\Delta_{LS2} = \Delta_{yi} + (0.0174/l_w - 2\epsilon_y/l_w)L_p + H_i \tag{13.16}$$

$$\Delta_{LS3} = \Delta_{yi} + (0.0720/l_w - 2\epsilon_y/l_w)L_p + H_i \tag{13.17}$$

Where H_{CF} stands for the height of the contra-flexure, amd L_p is the plastic hinge length given by the following equation:

$$L_p = kH_CF + 0.1l_w + 0.0022f_yd_{bl} \tag{13.18}$$

Where l_w is the wall lenght, d_bl is the diameter of the vertical rebars and k is equal to $0.2(f_u/f_y - 1) \leq 0.08$ where f_u and f_y are equal to the the ultimate and yield strength of the steel respectively.

The estimation of the effective height for dual frame-wall structures proved to be more challenging due to the fact that it is common to occur both beam- and column-sway mechanisms simultaneously. For a pure beam-sway mechanism, an effective height ratio of 0.7 can be used while for a pure column-sway mechanism, an effective height ratio equal to 0.5 can be assumed [Priestley et al., 2007]. Bal et al. [2010] conducted several analysis with the purpose of estimating the contribution of the frames to the total base shear (represenred by β_{MF} and the relationship between the total height of the building and the respective effective and contra-flexure height. A normal distribution was fit to these values and the mean and coefficient of variation are presented in table 13.3.

Table 13.3.: Parameters for the assessment of dual wall-frame structures

Parameter	Mean	COV	Lower-Upper Bounds
β	0.12	0.6	0.04 - 0.40
H_{CF}/H_n	0.50	0.50	0.10 - 1.00
H_{eff}/H_n	0.61	0.11	0.50 - 0.70

Regarding the limit state periods, studies carried out by Vuran et al. [2008] and Bal et al. [2010] pointed to a yield period equal to $0.075H_T$

13.3.2. Masonry Buildings

Masonry buildings reveal a structural behavior distinct from what was observed in reinforced-concrete buildings due to their heterogeneity regarding construction materials and structural elements.

For the assessment of masonry buildings, two seismic response mechanisms can be considered:

- Global Mechanism: Occurs when buildings have have enough structural integrity to provide seismic resistance predominantly through the development of in-plane/out-of-plane deformations in structural walls;

- Local Mechanism: Occurs in buildings with lack of structural robustness in which the seismic response of the structural walls are characterized by a out-of-plane failure.

Regarding the first response mechanism, Restrepo-Velez and Magenes [2004] proposed the following formula:

$$\Delta_{LS} = \theta_y k_1 H_T + k_2(\theta_{LS} - \theta_y)h_s \tag{13.19}$$

Where θ_y stands for the inter storey yield drift, k_1 and k_2 represent the displacement coefficients to convert multi degree of freedom (MDOF) structural systems into an equivalent single degree of freedom (SDOF) system, θ_{LS} stands for the second or third limit state inter storey drift h_s stands for the pier height. Values for k_1 and k_2 as a function of the number of storeys can be found in [Restrepo-Velez and Magenes, 2004]. Regarding the inter storey drift for the different limit states, [Ahmad et al., 2011] studied the structural behavior of Stone and Brick masonry buildings, proposing the estimates presented on Table 13.4.

Table 13.4.: Parameters for the assessment of masonry buildings

Parameter	Mean	COV	Lower-Upper Bounds	Probability Distribution
$\theta_{LS1}(all)$	0.079	0.104	0.064 - 0.096	Truncated Lognormal
$\theta_{LS2}(all)$	0.099	0.102	0.08 - 0.12	Truncated Lognormal
$\theta_{LS3}(B-H)$	0.2944	0.114	0.24 - 0.36	Truncated Lognormal
$\theta_{LS4}(B-H)$	0.4418	0.114	0.36 - 0.54	Truncated Lognormal
$\theta_{LS3}(B-L)$	0.471	0.113	0.384 - 0.5759	Truncated Lognormal
$\theta_{LS4}(B-L)$	0.7084	0.113	0.576 - 0.864	Truncated Lognormal
$\theta_{LS3}(SM)$	0.4002	0.114	0.3253 - 0.488	Truncated Lognormal
$\theta_{LS4}(SM)$	0.5992	0.114	0.488 - 0.732	Truncated Lognormal

Note that [Ahmad et al., 2011] used 4 limit state instead of 3 like previous authors. In Table 13.4, the first and second limit state drift are common to all the masonry building typologies while for the third and forth limit state, specific values were computed for each typology (B-H: brick masonry high rise, B-L: brick masonry low rise, SM: stone masonry).

PART IV

Socio-Economic Impact Assessment

PART V

Modeller's Toolkit

CHAPTER 14

Introduction

Introduction to the hazard input Modellers' Toolkit

CHAPTER 15

Input visualization and preparation

15.1. Hazard

15.2. Risk

15.3. Socio-Economic Impact

PART VI

Appendixes

APPENDIX A

nrML

This is the nrML introduction

```
<?xml version="1.0" encoding="UTF-8"?>
</ns2:logicTreeSet>
```

Figure A.1.: nrML example

APPENDIX B

Example of OpenQuake risk calculation configuration file

This is a test

Bibliography

Abrahamson, N. A. and SIlva, W. (2008). Summary of the abrahamson & silva nga ground-motion relations. *Earthquake Spectra*, 24(1):67–97.

Ahmad, N., Crowley, H., and Pinho, R. (2011). Analytical fragility functions for feinforced concrete and masonry buildings and building aggregates of euro-mediterranean region. Technical report, Department of Structural Mechanics, University of Pavia.

Aki, K. and Richards, P. G. (2002). *Quantitative Seismology*. University Science Books, Sausalito, California.

Atkinson, G. A. and Boore, D. M. (2006). Earthquake Ground-Motion Prediction Equations for Eastern North America. *Bulletin of the Seismological Society of America*, 96(6):2181–2205.

Bal, I., Crowley, H., and Pinho, R. (2010). *Displacement-Based Earthquake Loss Assessment: Method Development and Application to Turkish Building Stock*. PhD thesis, Centre for Post-Graduate Training and Research in Earthquake Engineering and Engineering Seismology.

Bender, B. and Perkins, D. M. (1982). SEISRISK II : a computer program for seismic hazard estimation. Open-File Report 82-293, United States Department of the Interiors, Geological Survey.

Bender, B. and Perkins, D. M. (1987). Seisrisk III: A computer program for seismic hazard estimation. Bulletin 1772, United States Geological Survey.

Bommer, J. J. and Scherbaum, F. (2008). The Use and Misuse of Logic Trees in Probabilistic Seismic Hazard Analysis. *Earthquake Spectra*, 24(4):997–1009.

Boore, D. M. and Atkinson, G. M. (2008). Ground-Motion Prediction Equations for the Average Horizontal Component of PGA, PGV, and 5%-Damped PSA at Spectral Periods between 0.01 s and 10.0 s. *Earthquake Spectra*, 24(1):99–138.

Calvi, G. M. (1999). A displacement-based approach for the vulnerability evaluation of classes of buildings. *Journal of Earthquake Engineering*, 26:1091–1112.

Chiang, W. L., Guidi, G. A., Scoof, C. G., and Shah, H. C. (1984). Computer Programs for Seismic Hazard Analysis - A User Manual (STASHA). Report 62, The J. A. Blume Earthquake Engineering Center.

Chiou, B. S.-J. and Youngs, R. R. (2008). An nga model for the average horizontal component of peak ground motion and response spectra. *Earthquake Spectra*, 24:173–215.

Coppersmith, K. J., Youngs, R. R., and Sprecher, C. (2009). Methodology and main results of seismic source characterization for PEGASOS Project, Switzerland. *Swiss J. Geosc.*, 102:91–105.

Cornell, C. A. (1968). Engineering seismic risk analysis. *Bulletin of the Seismological Society of America*, 58:1583–1606.

Crowley, H. and Pinho, R. (2004). Period-height relationship for existing european reinforced concrete buildings. *Journal of Earthquake Engineering*, 8:93–120.

Crowley, H. and Pinho, R. (2006). Simplified equations for estimating the period of vibration of existing buildings. In *Proceedings of the 1st European Conference on Earthquake Engineering and Seismology, Geneva, Switzerland, paper no 1122*.

Crowley, H., Pinho, R., and Bommer, J. (2004). A probabilistic displacement-based vulnerability assessment procedure for earthquake loss estimation. *Bulletin of Earthquake Engineering*, 2:173–219.

Crowley, H., Pinho, R., Bommer, J., and Bird, J. (2006). *Development of a Displacement-based Method for Earthquake Loss Assessment*. IUSS Press, Pavia, Italy.

Esteva, L. (1968). *Bases para la formulacion de decisiones de diseno sismico*. PhD thesis, Universidad Autonoma Nacional de Mexico.

FEMA-440:ATC (2005). Improvement of nonlinear static seismic analysis procedures,. Technical report, California, USA.

Field, E. H., Jordan, T. H., and Cornell, C. A. (2003). OpenSHA - A developing Community-Modeling Environment for Seismic Hazard Analysis. *Seism. Res. Lett.*, 74:406–419.

Frankel, A. (1995). Mapping Seismic Hazard in the Central and Eastern United States. *Seismological Research Letters*, 66(4):8–21.

Glaister, S. and Pinho, R. (2003). Development of a simplified deformation based method for seismic vulnerability assessment. *Journal of Earthquake Engineering*, 7:107–140.

Jayaram, N. and Baker, J. W. (2009). Correlation model for spatially distributed ground-motion intensities. *Earthquake Engineering and Structural Dynamics*.

Kumar, M. (2008). Development of period-height and displacement capacity equations for embedded beam structures. Master's thesis, Rose School, Italy.

McGuire, K. K. (1976). Fortran computer program for seismic risk analysis. Open-File report 76-67, United States Department of the Interior, Geological Survey. 102 pages.

McGuire, R. K. (2004). *Seismic Hazard and Risk Analysis*. EERI.

Pagani, M. and Marcellini, A. (2007). Seismic-hazard disaggregation: A fully probabilistic methodology. *Bulletin of the Seismological Society of America*, 97(5):1688–1701.

Pagani, M., Monelli, D., Crowley, H., Danciu, L., Field, E. H., Wiemer, S., and Giardini, D. (2010). GEM1 Hazard: Description of Input Models, Calculation Engine and Main Results. GEM Technical Report 2010-3, GEM Foundation, Pavia, Italy.

Paulay, T. and Priestley, M. J. N. (1992). *Seismic Design of Reinforced Concrete and Masonry Buildings*. John Wiley and Sons, Inc., New York.

Pinho, R., Bommer, J., and Glaister, S. (2002). A simplified approach to displacement-based earthquake loss estimation analysis. In *Proceedings of the 12th European Conference on Earthquake Engineering, London, UK, paper no 738*.

Priestley, M. J. N. (1997). Displacement-based seismic assessment of reinforced concrete buildings. *Journal of Earthquake Engineering*, 1:157–192.

Priestley, M. J. N., Calvi, G. M., and Kowalsky, M. J. (2007). *Displacement-based seismic design of structures*. IUSS Press, Pavia, Italy.

Restrepo-Velez, L. F. and Magenes, G. (2004). Simplified procedure for the seismic risk assessment of unreinforced masonry buildings. In *Proceedings of the 13th World Conference on Earthquake Engineering, Vancouver, Canada, Paper no.2561*.

Senior Seismic Hazard Analysis Committee (1997). Recommendations for probabilistic seismic hazard analysis: Guidance on uncertainty and use of experts. Technical Report NUREG/CR-6372, UCRL-ID-122160, Vol. 1, Lawrence Livermore National Laboratory.

Sullivan, T. J., Priestley, M. J. N., and Calvi, G. M. (2006). *Seismic design of frame-wall structures*. IUSS Press, Pavia, Italy.

Vuran, E., Bal, I., Crowley, H., and Pinho, R. (2008). Determination of equivalent sdof characteristics of 3d dual structures. In *Proceedings of the 14thWCEE, Beijing, China, paper no: S15-031*.

Wesson, R. L., Perkins, D. M., Luco, N., and Karaca, E. (2009). Direct calculation of the probability distribution for earthquake losses to a portfolio. *Earthquake Spectra*, 25(3):687–706.

Woo, G. (1996). Kernel estimation methods for seismic hazard area source modeling. *Bulletin of the Seismological Society of America*, 86(2):353–362.

Zhao, J. X., Zhang, J., Asano, A., Oyno, Y., Oouchi, T., Takahashi, T., Ogawa, H., Irikura, K., Thio, H. K., Somerville, P. G., Fukushima, Y., and Fukushima, Y. (2006). Attenuation relations of strong ground motion in japan using site classification based on predominant period. *Bulletin of the Seismological Society of America*, 96:898–913.